

# Hydrogeochemical Processes Associated with Double Salinization of Water in an Algerian Aquifer, Carbonated and Evaporitic

Abdelhamid Saou<sup>1\*</sup>, Mustapha Maza<sup>1</sup>, Jean Luc Seidel<sup>2</sup>

<sup>1</sup>Research Laboratory in applied hydraulics and Environment, University of Bejaia, Algeria

<sup>2</sup>UMR HydroSciences, University of Montpellier 2, France

Received: 15 February 2011

Accepted: 28 December 2011

## Abstract

For this study, geochemical data were examined to determine the main factors and mechanisms controlling the water chemistry and the salinity of low Soummam basin in Algeria. Parameters such as pH, EC, temperature, and major and minor element concentrations for two sampling campaigns at the extreme hydrological regimes were considered. The analytical results obtained were interpreted using in particular the molar ratios Na/Cl, Mg/Ca, SO<sub>4</sub>/Cl, B/Cl, Br/Cl, Li/SO<sub>4</sub>, and Sr/Ca, as tracers of hydrochemical evolution of water, saturation indexes, and the comparison between the chloride content and the other major and minor elements characterizing the salinization. The results obtained indicate the signature of seawater intrusion in the coastal zone and the influence of gypsum outcrops in the upstream zone.

**Keywords:** groundwater, surface water, double salinization, hydrochemical tracers, Soummam basin, Algeria

## Introduction

Salinity in coastal aquifers is a phenomenon that is highly widespread that causes progressively the salinization of groundwater. This phenomenon has been extensively studied by several authors, particularly in the Mediterranean basin, with the extension of semi-arid conditions, water overexploitation, and low recharge. The salinity increase is often attributed only to marine intrusion [1-9].

For the alluvial aquifer of the lower Soummam, understanding the processes and factors that control the evolution of water mineralization, and in particular salinity, is a complex task because the aquifer is fed from different origins:

- The Sahel Soummam and Boussellam rivers and their tributaries

- Hypodermic flow of the high Soummam aquifer and from the various thermal springs
- Its own catchment area
- Intrusion of seawater

The alluvial aquifer is exposed to the phenomenon of double salinization. During floods, water infiltration, in contact with rocks, acquires a mineral charge characteristic of leached evaporitic rocks and, during low-water periods, the draw-down of groundwater level in the water body causes an inversion of the hydraulic gradient or even a seawater intrusion.

In this paper the analysis of the major and trace elements in water were carried out in order to determine the origin of the high salinity of the low Soummam basin and to describe their spatial and temporal evolution. The water-rock interaction leading to the dissolution of carbonated and silicated minerals, and the deterioration of the processes of ion exchange, were investigated by sampling 32 sites, represented by boreholes and stations of surface water (Fig. 1).

---

\*e-mail: saouhamid@yahoo.fr

Our objective was to contribute to a better understanding of the process of increased mineralization through two sampling campaigns during high- and low-stage periods when the groundwater level in the aquifer and the rivers were at their extreme hydrological regimes. The influence of evaporitic formations, leaching occurring in the upstream of the basin, and of seawater intrusion in the downstream, were identified by the salinization of the waters of the mio-plio-quaternary aquifer of low Soummam.

### Study Area Description

The area of study is located in eastern Algeria, characterized by a wet climate and average precipitation and temperature of about 750 mm/year and 18°C. This studied area is situated in the alluvial plain of the Mio-Plio-Quaternary. The aquifer is directly fed by stream water coming from different reliefs surrounding the depression, inter-mountainous of the low Soummam valleys. The rivers of the region, locally called "Oued;" have an intermittent flow regime because the annual dry season is typically very long (6-7 months). The main Oued in this basin is the Soummam River, which receives many important flow tributaries, in particular from the high Akfadou-Taourirt Ighil mountains (Oued Remila) in the west, Gouraya-Aghbalou mountains (Oued El-Kseur, Oued Ghir) in the north, and the Babors mountains (Oued Amassine, Oued Amizour) in the south (Fig. 1).

### Geology and Hydrogeology Settings

The coastal plain of low Soummam covers a surface area of 709 km<sup>2</sup>. This plain is an alluvial depression between the northern Tell and the southern Tell. It has a

great complexity due to the superposition of geological units that characterize the geology of northern Algeria [10-12]. The sedimentary series range from the Triassic to the Quaternary. Triassic deposits outcrop in the west and south of the region. The gypsum and halite associated with variegated clays are the predominant minerals in the Triassic formation. In the south, Jurassic and Cretaceous formations are mainly observed in the Babors Mountains. In the north, these formations are observed in the Gouraya-Aghbalou and Akfadou-Taourirt Ighil Mountains. The Jurassic formation is formed by limestone, dolomite, shale, and marl. The Cretaceous formation is subdivided into two:

- (1) Neocomian is formed by limestone, marl, and shale
- (2) Aptian consists of flyschs, sandstone, quartzite, and green shale

In the north, these formations are observed in the Gouraya-Aghbalou Mountains. The Miocene-pliocene formation consists of limestone, sandstone, clay, and conglomerate. In the studied area the aquifer is composed of Quaternary detrital sediments. These sediments (conglomerates, gravels, sands, and silts), deriving from the rapid erosion of the Soummam River, were carried down by rivers and washes, and range widely in grain size, from large gravels to clays and silts. The piezometric survey shows a flow direction from west to east toward the Mediterranean Sea, which constitutes the main outlet of the Soummam aquifer (Fig. 1). The major drainage axis appears along the Soummam River. Generally, the aquifer has good hydrodynamic characteristics [2]. The highest permeability values, reaching  $5.1 \cdot 10^{-4}$  m/s, are found in the western zone. Lower values are found in the eastern zone. Transmissivity varies continuously from upstream to the coastal zone, ranging from  $1.98 \cdot 10^{-3}$  to  $7.5 \cdot 10^{-2}$  m<sup>2</sup>/s.

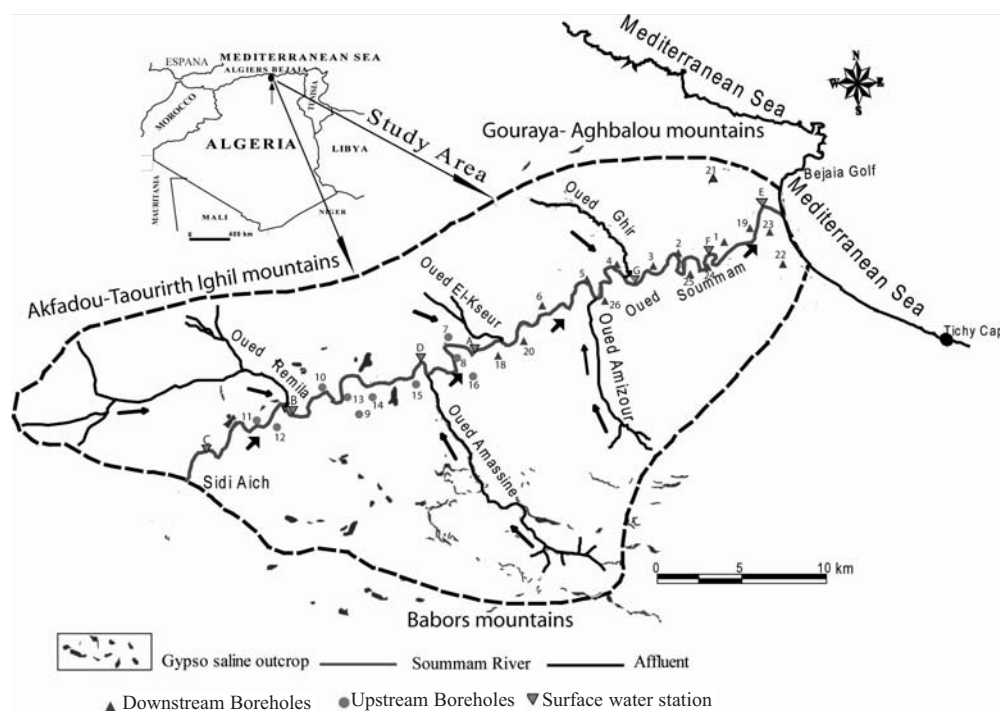


Fig. 1. Hydrographic situation, distribution of the gypso-saline formations and sampling points: boreholes and surface stations in the valley of low Soummam, Bejaia (Algeria).

The highest values are found in the west (from Sidi Aich to Oued Ghir), whereas the lowest are measured in the east (from Oued Ghir to sea).

## Materials and Methods

A total of 25 groundwater samples from 8 irrigation boreholes: 17 boreholes used for human consumption derived from the Quaternary alluvial aquifer and seven river samples (Fig. 1) were collected. In order to remove any stagnant water in boreholes, samples were collected after a pumping time as long as possible until the electrical conductivity (EC) and pH values had stabilized. River water samples were collected from a bridge below the water surface in turbulent areas where the water column was well mixed [13]. Temperature, pH, and electrical conductivity were measured in situ using portable instruments (EXSTIK II pH/conductivity EC. 500). All chemical analyses were carried out at the HydroSciences Montpellier laboratory (University of Montpellier 2, France). Alkalinity was measured using acid-base titration. Samples were first filtered through 0.45  $\mu\text{m}$  membrane filters, with samples for minor and trace elements acidified using concentrated analytical-grade  $\text{HNO}_3$  to prevent adsorption and chemical precipitation. All water samples were stored at 4°C until analysis. The analyses of major and minor ions (Br, Cl,  $\text{NO}_3^-$ ,  $\text{SO}_4^{2-}$ , Na, K, Mg, and Ca) were performed using ion chromatography (DIONEX<sup>®</sup> – ICS-1000). Other minor elements and trace elements (Li, B, Al, V, Cr, Mn, Fe, Co, Ni,

Cu, Zn, Rb, Sr, Mo, Cd, Sn, Cs, Ba, Pb, and U) were analyzed using inductively coupled plasma-mass spectrometry (ICP-MS X Series 2 Thermo Scientific<sup>®</sup>).

## Results and Discussion

### Surface and Groundwater Chemistry

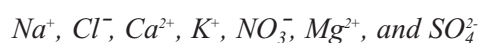
Physicochemical parameters, the major and trace element concentrations for the water samples, collected respectively in April and September 2009, are listed in Tables 1 and 2. Typical ratios of major and trace elements for high and low water stages are shown in Tables 3 and 4. These waters are dominated by  $\text{Na}^+$ ,  $\text{Ca}^{2+}$ ,  $\text{Cl}^-$ , and  $\text{SO}_4^{2-}$ . Mention should be made of the high values of electrical conductivity (2550–4180  $\mu\text{S}/\text{cm}$ , and high concentrations for  $\text{Cl}^-$  (13.6–73.6 meq/L),  $\text{Na}^+$  (13.6–59 meq/L),  $\text{SO}_4^{2-}$  (7.7–26.5 meq/L), and  $\text{Ca}^{2+}$  (9.5–39.4 meq/L) in upstream boreholes during high water periods (Table 1). During low water periods, the high concentrations of these elements were observed in upstream and downstream boreholes and in river water (Table 2).

The relationship of anions and cations of the low Soummam water (high and low water periods) is shown in Fig. 3. The calcite, dolomite, and gypsum saturation indices as a function of  $\text{SO}_4$  concentration in surface and groundwater (high and low water periods) are illustrated in (Fig. 4). The relationship between the main components characterizing the salinity of the low Soummam water (high and low water periods) is illustrated in (Fig. 5).

### Hydrochemical Facies

Surface and groundwater samples were plotted on a Piper diagram (Fig. 2). On the basis of dominant anions through the high and low water periods, two hydrochemical facies in groundwater were determined, namely: upstream of Oued Ghir, a reservoir of ( $\text{Na}^+ > \text{Ca}^{2+} > \text{Mg}^{2+} > \text{K}^+$ )-type was identified. Downstream (from Oued Ghir to the sea), a reservoir of ( $\text{Ca}^{2+} > \text{Na}^+ > \text{Mg}^{2+} > \text{K}^+$ )-type was identified. In the Soummam river water, only ( $\text{Na}^+ > \text{Ca}^{2+} > \text{Mg}^{2+} > \text{K}^+$ )-type was identified. On the basis of dominant cations and anions, five water types were found for water samples:  $\text{Cl}^- > \text{Na}^+$ ,  $\text{HCO}_3^- > \text{Ca}^{2+}$ ,  $\text{SO}_4^{2-} > \text{Na}^+$ ,  $\text{SO}_4^{2-} > \text{Ca}^{2+}$ , and  $\text{HCO}_3^- > \text{Na}^+$ , each representing 50, 28.1, 25, 9.25, and 6.25% of the total of water samples analyzed. The  $\text{Cl}^- > \text{Na}^+$ -type water is dominant in most of the study area.

### Hydrochemical Results



In order to identify the sources of each element during the concentration process, the data are presented in concentration diagrams built using conservative tracers to estimate the concentration factor. Chloride is usually considered as a conservative tracer and the relation between chloride and the

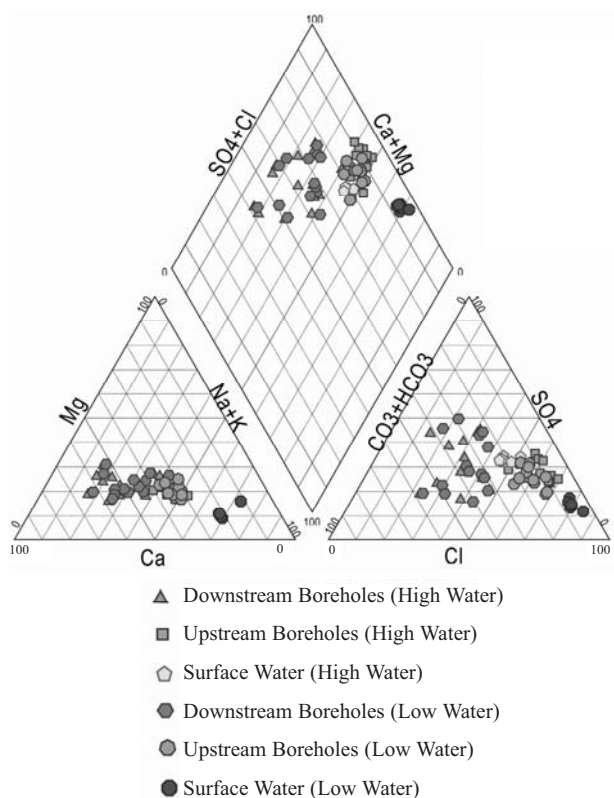


Fig. 2. Piper diagram for surface and groundwater of the valley of Soummam (high and low water periods).

Table 1. Concentrations of major and trace elements characterizing salinity (April 2009).

	No.	T	pH	EC	HCO <sub>3</sub> <sup>-</sup>	Cl <sup>-</sup>	SO <sub>4</sub> <sup>2-</sup>	Ca <sup>2+</sup>	Mg <sup>2+</sup>	Na <sup>+</sup>	K <sup>+</sup>	NO <sub>3</sub> <sup>-</sup>	Br <sup>-</sup>	Sr	B	Li
		°C		µS/cm	meq/L	meq/L	meq/L	meq/L	meq/L	meq/L	meq/L	meq/L	meq/L	µg/L	µg/L	µg/L
Downstream boreholes	1	18.2	6.8	2500	8.5	12.2	5.4	12.4	5	10.5	0.01	0.98	5.26E-02	2271	162.6	32.1
	2	19.1	6.7	1640	8.9	4.8	4.2	9.3	3.5	5.5	0.02	0.23	5.01E-02	1619	117.6	9.7
	3	18.6	6.7	2370	6.9	8.5	12	14.5	6.3	7.4	0.07	0	5.26E-02	2658	181	48.4
	4	20.5	6.9	1467	9.6	3.9	3.1	9.7	4.1	3.3	0.01	0.07	4.51E-02	1524	105.2	9.8
	5	21.1	7.6	2460	5	12.8	8.3	10.3	5.7	10.8	0.04	0.15	8.39E-02	3043	144.8	46.5
	6	20.5	6.9	1835	6.1	7.9	4.8	8.9	4.2	6.5	0.05	0.29	6.51E-02	2030	112.6	31.6
	19	18.5	7.1	2500	9	8.2	8.7	11	8	10.5	0.29	2.82	7.51E-02	2888	281	36.3
	20	17.4	6.8	1717	6	5.2	7.5	10.4	5.1	4.4	0.01	0.5	3.25E-02	1204	101.1	13.8
	21	16.5	6.8	1142	7.2	2.9	2.3	8.5	2.4	2.2	0	0.15	3.63E-02	1075	122.6	4.7
	22	16.5	7	874	3.8	1.3	4	5.5	2.5	1.5	0.02	0.05	4.88E-02	935.5	25.1	7.2
	23	17.6	7.3	1353	5.7	4.9	4.1	5.5	4	6	0	0.15	6.13E-02	1179	150.1	12.6
	24	16.3	7	1770	8.2	7.1	3	10.5	6	3.2	0.02	0.77	7.88E-02	2899	148.4	15.9
	25	17.6	6.8	996	3.7	2.3	3.8	5.7	2	3	0.02	0	1.63E-02	323.5	35.2	6.6
	26	16.2	7.3	1838	5	6.8	9.6	12.8	3.5	5.5	0.07	0	3.63E-02	1618	93.6	14.1
Upstream boreholes	7	20.1	6.9	3220	5.8	41	14.4	22.2	13.4	32.7	0.13	0.45	5.13E-02	3986	190.6	99.8
	8	20.1	7.2	3330	5	44.7	17.9	26.2	15.7	32.5	0.17	0.26	4.63E-02	4241	174.6	92.1
	9	20.5	6.8	2550	5.9	13.6	7.9	9.5	4.7	13.9	0.07	0.06	6.88E-02	2292	146	64
	10	21.8	6.9	3130	5.4	36.7	13.4	21.4	10.4	30	0.1	0.33	4.26E-02	3206	175.6	81.9
	11	20.6	6.8	3360	6.2	39.5	24.9	28.9	17.4	33.1	0.09	0.23	4.88E-02	4885	206	79.6
	12	17.8	7	3100	5.1	33.2	18.9	25.7	13	24.9	0.05	1.41	4.26E-02	3865	190.3	63
	13	19	6.9	2840	5.3	17.2	7.7	11.4	5.8	13.8	0.06	0.14	8.51E-02	3355	164.9	79.2
	14	20.4	6.7	3410	7.5	41.6	18.4	27.7	16.9	33	0.11	1.33	3.63E-02	3472	193.9	120.1
	15	18.1	6.9	4180	6.4	73.6	26.5	39.4	23.1	59	0.17	1.29	2.63E-02	3681	200.3	102.7
	16	19	6.9	3940	5.6	45.7	24.8	26.3	18.2	38.5	0.09	7.08	5.26E-02	4877	172.6	77.8
18	19.5	7.1	2910	5.2	16.8	9.9	11.4	7.2	20.6	0.07	6.51	1.03E-01	4058	176.6	76.3	
Surface water	A	19.2	7.9	1731	3.7	8.1	6.1	6	3.9	8.6	0.08	0.09	1.00E-01	2072	142.6	89.3
	B	20.2	7.7	1716	3.8	8	5.6	5.8	3.7	8.2	0.08	0.07	1.01E-01	2043	145.8	93.1
	C	20.3	7.5	1847	3.9	8.9	6	6.2	4	8.9	0.09	0.07	1.00E-01	2192	153.4	100.5
	D	20.3	7.8	2090	4.1	14.5	9.5	9.2	6.1	14.9	0.12	0.1	7.26E-02	2324	168.8	111.7
	E	16.9	7.6	1966	3.9	10	6.5	6.6	4.3	10.1	0.09	0.12	9.64E-02	2226	160.4	103.2
	F	16.4	7.7	1439	3.5	7.4	5.3	5.8	3.6	7.7	0.09	0.09	8.13E-02	1657	120.3	70.5
	G	14.9	7.7	1514	3.5	6.9	5	5.4	3.4	7.2	0.08	0.09	9.14E-02	1707	123.2	71.6

other major and trace elements dominating chemical compositions of surface and groundwater for high and low stage data contributes to better understand the processes of the mineralization increase. The relation Na-Cl is often used to identify the mechanisms of acquisition of salinity and marine intrusion. Na<sup>+</sup> is higher and positively correlated with Cl<sup>-</sup> ( $r=0.981$  and  $r=0.994$ , respectively for high and

low waters (Fig. 3a)), in periods of high waters, the majority of the samples are grouped along the straight line of Soummam water dilution (conservative line) and plot very close to or slightly above the SW dilution. In periods of low waters, most of the samples plot close to or below the conservation line and plot very close to or slightly above the SW dilution, which suggests double salinization by seawater

Table 2. Concentrations of major and trace elements characterizing salinity (September 2009).

	No.	T	pH	EC	HCO <sub>3</sub> <sup>-</sup>	Cl <sup>-</sup>	SO <sub>4</sub> <sup>2-</sup>	Ca <sup>2+</sup>	Mg <sup>2+</sup>	Na <sup>+</sup>	K <sup>+</sup>	NO <sub>3</sub> <sup>-</sup>	Br <sup>-</sup>	Sr	B	Li
		°C		µS/cm	meq/L	meq/L	meq/L	meq/L	meq/L	meq/L	meq/L	meq/L	meq/L	µg/L	µg/L	µg/L
Downstream boreholes	1	16	6.69	2050	7.18	10.18	4.42	9.9	4.45	8	0.03	0.45	1.37E-02	1 886	161.5	26.98
	2	16.1	6.75	1622	8.72	5.26	4.03	9.14	3.62	5.67	0.03	0.09	8.68E-03	1 637	127.6	10.42
	3	12.9	6.75	2220	6.4	8.37	11.11	12.81	5.36	7.16	0.1	0	6.39E-03	2 401	175.9	45.11
	4	14.2	6.85	1362	7.16	4.68	2.78	8.16	3.17	3.82	0.02	0.12	5.51E-03	1 034	87.56	4.17
	5	20.8	7.56	2310	8.14	10.38	6.85	10.64	6.29	8.8	0.1	0	7.94E-03	2 362	128.2	44.87
	6	11.5	6.86	1839	6.16	8.23	4.95	8.85	4.35	6.55	0.06	0.3	6.84E-03	2 108	123.2	28.87
	19	12.4	7.2	2210	8.9	8.45	7.58	9.71	6.93	8.64	0.19	0.08	1.32E-02	3 276	400.4	34.57
	20	23.2	6.84	2080	5.46	8.46	8.59	10.3	5.64	6.89	0.04	0.5	5.93E-03	1 500	119.4	16.46
	21	12.7	6.84	1123	7.14	3.01	2.41	8.04	2.55	2.35	0.01	0.13	4.44E-03	1 077	138.4	4.08
	22	14.7	6.99	945	3.84	1.88	4.79	5.68	2.82	1.87	0.04	0.03	1.27E-03	2 187	71.84	13.67
	23	18.1	7.34	1065	4.24	4.2	3.28	3.91	3.29	4.96	0.23	0.05	7.29E-03	1 888	278.1	17.84
	24	14.3	7.1	1820	7.9	8.43	3.05	10.38	6.16	3.44	0.01	0.37	6.27E-03	6 055	324.6	24.8
	25	14.5	6.82	1188	3.7	2.76	6.35	6.95	2.36	3.25	0.06	0.34	3.86E-03	895	89.22	11.63
	26	23.7	7.35	1860	4.96	7.05	9.49	11.87	3.56	5.48	0.07	0.02	8.12E-03	4 447	239.7	26.89
Upstream boreholes	7	14.4	6.93	2800	7	16.87	7.13	8.88	5.85	14.34	0.1	0.19	6.27E-03	3 312	192	84.41
	8	23.8	7.2	3170	3.18	21.15	8.52	11.59	7.23	15.41	0.12	0.13	6.66E-03	4 457	206	91.96
	9	22.7	6.83	4260	6	30.84	8.58	14.78	7.69	23.26	0.13	0.09	9.03E-03	4 338	258.7	135.2
	10	16.1	6.86	3710	4.82	26.42	7.7	13.72	7.41	18.64	0.11	0	8.39E-03	4 288	206.9	99.19
	11	16.5	6.9	3440	6.06	20.2	12.19	13.52	8.54	16.18	0.08	0.1	8.53E-03	5 080	239.8	71.07
	12	15.8	6.97	3030	5.1	18.45	9.03	12.09	7.38	13.07	0.06	0.26	8.33E-03	4 658	219.4	69.67
	13	21.1	6.85	3180	5.06	20.84	7.98	12.31	6.63	15.42	0.09	0.13	6.92E-03	3 965	186.1	78.66
	14	23.3	6.71	3190	6.92	19.63	9	12.27	8.3	14.74	0.08	0.53	8.00E-03	3 835	198.3	81.23
	15	14.6	6.93	3790	5.48	23.82	13.42	13.66	9.94	21.2	0.09	0.33	8.23E-03	4 960	187.2	66.55
	16	21.9	6.92	3660	6.58	23.14	9.38	12.03	7.16	19.21	0.08	0.47	9.50E-03	3 227	212.8	83.49
18	16.1	7.05	3000	4.58	18.46	9.77	9.16	7.79	14.21	0.08	0.17	6.21E-03	3 899	188.8	68.18	
Surface water	A	17	7.5	6450	4.06	54.98	12.27	15.35	7.2	47.97	0.35	0.14	1.51E-02	5 968	590.5	544.2
	B	16.5	7.73	5520	3.46	44.19	8.13	12.33	5.27	38.92	0.33	0.14	1.25E-02	4 303	491.5	469.9
	C	16.3	7.47	5840	4.72	52.41	8.76	14.13	5.88	45.57	0.34	0.1	1.30E-02	4 963	554.3	571.5
	D	13.8	7.76	6820	3.8	47.35	8.44	12.93	5.76	40.92	0.33	0.17	1.23E-02	4 615	533.4	533.4
	E	14.4	7.6	6670	4.5	108.58	15.17	14.77	20.54	92.27	1.5	0	1.11E-01	5 129	981.4	440.7
	F	16.4	7.55	6010	4.44	48.11	9.64	13.63	6.84	42.06	0.31	0.12	1.32E-02	4 669	509.7	494.3
	G	15	7.6	11080	4.34	54.98	10.27	15.3	7.69	47.71	0.37	0.12	1.36E-02	2 624	296.2	302.2

ter and the dissolution of halite related to the presence of saliferous rocks within the Mio-Plio-Quaternary alluvial sediments in the upstream part. This pattern is confirmed by low Na<sup>+</sup>/Cl<sup>-</sup> molar ratios, ranging from 0.45 to 1.30 and from 0.41 to 1.18 for respectively high and low water periods (Tables 1 and 2). Nitrate values are relatively low, ranging from 0 to 7.08 and from 0 to 0.53 meq/L for respec-

tively high and low water periods. The high values are detected in the upstream area, where industrial and agricultural activities are intense.

In literature, the SO<sub>4</sub><sup>2-</sup>/Cl<sup>-</sup> ratio generally decreases with the increase of the salinity of water and Mg<sup>2+</sup>/Ca<sup>2+</sup> ratio increases proportionally with the increase of salinity [13-16]. We notice through the two campaigns covering the

complete hydrological cycle that  $SO_4^{2-}/Cl^-$  ratio varies from 0.35 to 3.08 and from 0.14 to 2.55 for respectively high and low water periods (Tables 1 and 2). The strongest values of  $SO_4^{2-}/Cl^-$  ratio are observed in the central part of the low Soummam, far from the coastal area and of the upstream influence, showing the double (marine and evaporitic) origin of water mineralization.  $Mg^{2+}/Ca^{2+}$  ratio varies from 0.275 to 0.737 and from 0.3 to 1.30 for, respectively, high and low water periods, and increases with an increase of water salinity. The strongest values are observed in the upstream and the downstream basin and are the smallest in the central part of the area. The assumption of natural contamination by seawater and triassic formations were confirmed by the high values of  $Mg^{2+}/Ca^{2+}$  ratio and by the low values of  $SO_4^{2-}/Cl^-$  (the opposite exchanges involve the capture of  $Na^+$  and  $Ca^{2+}$  ions by the substratum clays) [7, 17]. The strong and positive correlations of  $Cl^-$  and  $K^+$  ( $r = 0.957$  and  $0.887$ ), and  $Cl^-$  and  $SO_4^{2-}$  ( $r = 0.88, 0.662$ ), respectively, high and low water periods likely indicate the dissolution of evaporite (KCl) and/or infiltration of fertilizers applied in the form of potash (KCl) and sulfate salts.

The dominant surface and groundwater type is sodium chlorurated. If the salt water intrudes the aquifer,  $Na^+$  is adsorbed on the clay fraction,  $Ca^{2+}$  is released and, consequently, the CaCl water type should be developed [6]. However, the salinization phenomenon occurred here in the upstream and downstream zones, but the CaCl water type has not been developed (Fig. 3b), with only a small amount during flood (high water period). This phenomenon suggests that the low Soummam basin zone presents the earlier stage of salinization; thus, the development of NaCl to CaCl water type has not yet been achieved and supports the idea that water infiltration, in contact with rocks acquires a mineral charge characteristic of leached evaporitic rocks. This idea is also confirmed by the relationship between Na vs (Ca+Mg) (Fig. 3c), indicating that samples plot below the Soummam water dilution.

The relationship between Mg vs Cl (Fig. 3d), indicates that samples plot above the fresh-seawater mixing line. This suggests other sources for Mg and Ca enrichment. The dissolution of gypsum and carbonates in the unsaturated zone is the probable factor increasing  $Ca^{2+}$  and  $Mg^{2+}$  in groundwater.

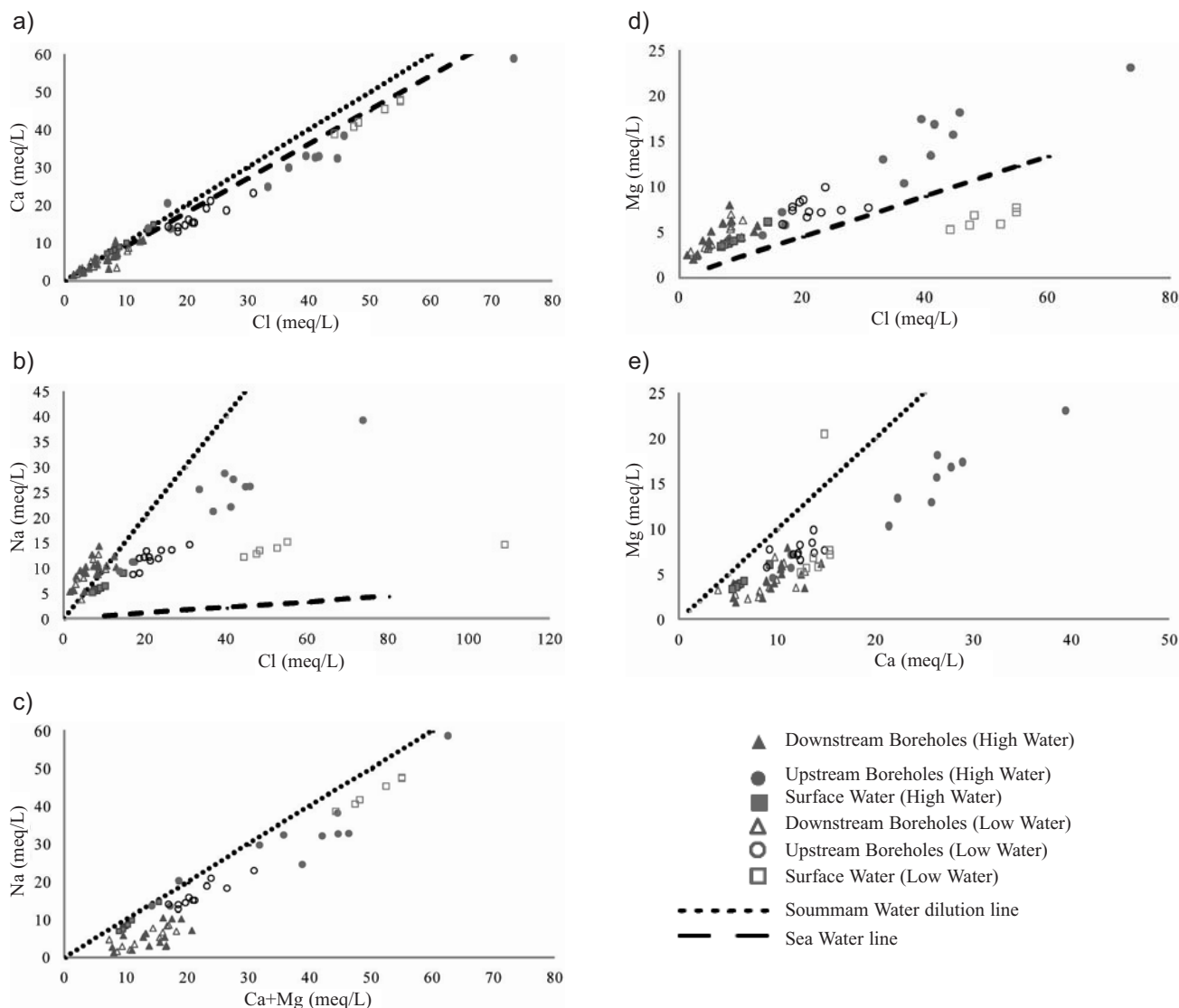


Fig. 3. Relationships among anions and cations of the low Soummam water (high and low water periods).

The very strong positive correlation between  $Mg^{2+}$  and  $Ca^{2+}$  ( $r = 0.943$ ) (Fig. 3e) during high water period could suggest that the dissolution of carbonate (calcite and dolomite) is an important process of control of  $Ca^{2+}$  and  $Mg^{2+}$  concentrations in the groundwater.  $CO_2$  enrichment of the water infiltrated in the aquifer promotes the dissolution of carbonate released in the solution of  $Ca^{2+}$  and  $HCO_3^-$  ions [18]. However, there is no relationship between  $Ca^{2+}$  and  $HCO_3^-$ , and the correlation coefficient is not significant. This indicates that calcite may not be a unique source of  $Ca^{2+}$ . On the other hand, the weak correlation of  $Mg^{2+}$  versus  $Ca^{2+}$  ( $r = 0.364$ ) (Fig. 3e) during low water period and the low  $Ca^{2+}$  and  $Mg^{2+}$  contents are due primarily to the absence of the contribution of water coming from leaching of the carbonated rocks.

Finally, we observe small additional Ca,  $SO_4$ , and Mg amounts due to dissolution of evaporite (only during high water period) coming from leaching of the carbonated rocks, located at the upstream basin and the salinization phenomenon that occurred in the entire study area. This fact suggests that calcite, dolomite and gypsum are the minerals precipitated from evaporating seawater in the earlier stage. The process of precipitation/dissolution in the alluvial aquifer of low Soummam is confirmed by the saturation index (SI), (Fig. 4) showing calcite, dolomite, gypsum, and strontianite saturation index as a function of sulphate concentration (high and low water data). The  $SO_4^{2-}$  concentration of surface and groundwater samples can be used to follow the extent of gypsum dissolution. Groundwater is mainly saturated or slightly super-saturated in respect to calcite and dolomite throughout the aquifer (Figs. 4a, 4b). For gypsum, the saturation state ranges from sub-saturation to near-equilibrium (Fig. 4c). For strontianite, the saturation state ranges near-equilibrium (Fig. 4d), indicating that  $SrCO_3$  is not the principal source of the Sr.

### Hydrochemical Tracers

#### *B/Cl, Br/Cl, Li/SO<sub>4</sub>, and Sr/Ca Molar Ratios*

The concentrations of boron and chloride in groundwater for the two campaigns were used to differentiate the marine influence for the B origin. The relationship between B vs Cl (Fig. 5a) shows that in a period of high waters, only boreholes of the downstream part are grouped along the line of seawater (SW) dilution, suggesting that seawater is the main source of boron. For low water period, SW influence is more pronounced; almost all samples are grouped along the SW dilution line. To better constrain this influence, we have considered the chloride ion. This ion is fundamentally related to seawater, and consequently the B/Cl ratio was used to determine the marine influence for boron. The high boron concentration in seawater is generally considered as an indication of marine intrusion processes. Nonetheless, in some cases the elevated boron content is related to the influence of other types of salinization, or contamination from anthropogenic origin associated with urban wastewaters [4]. In high water period (Fig. 5b), most

samples of the upstream boreholes are below the seawater dilution line, suggesting dissolution of evaporite as confirmed by Br/Cl ratios. These samples plot in the halite dissolution field, but samples of surface and groundwater are near or above the seawater dilution line, suggesting a pos-

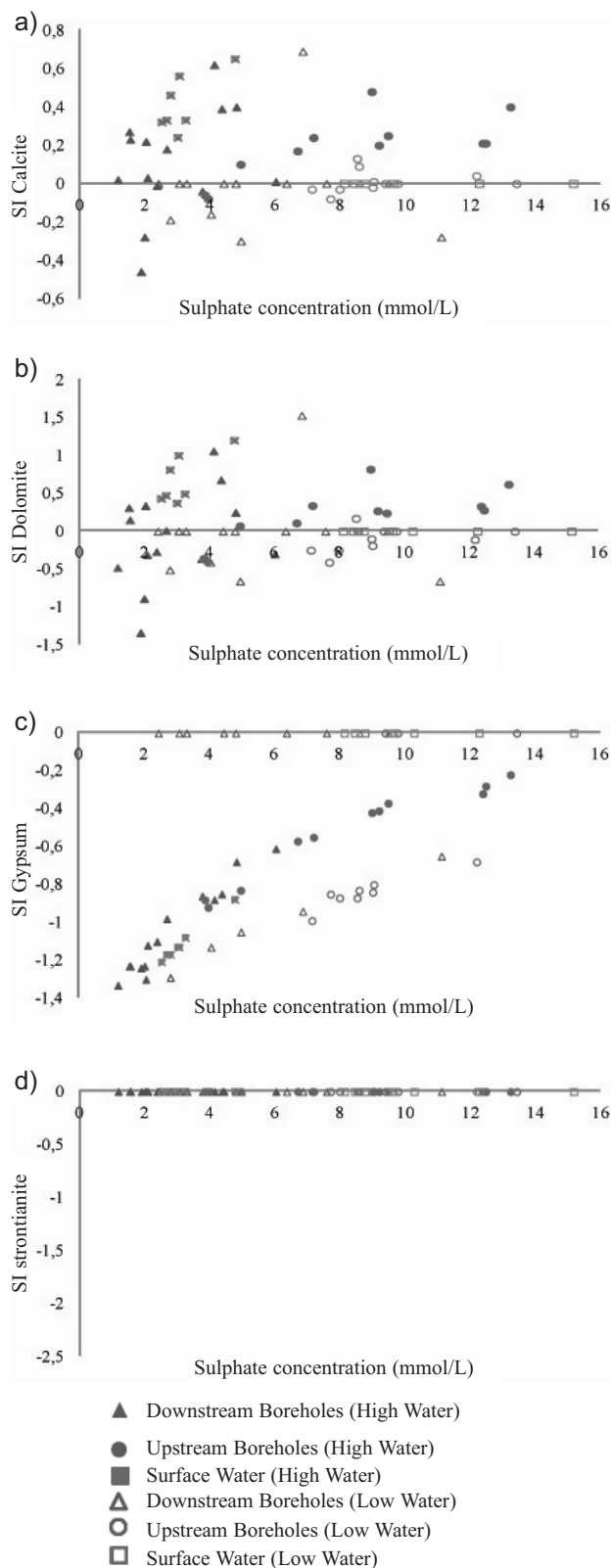


Fig. 4. Calcite, dolomite, gypsum, and strontianite saturation indices as a function of  $SO_4$  concentration in Soummam water (high and low water periods).

Table 3. Typical ratios of major and trace elements characterizing salinity (April 2009).

	No.	Na/Cl	Sr/Ca	B/Cl	Mg/Ca	SO <sub>4</sub> /Cl	Li/SO <sub>4</sub>	Br/Cl
		(molar)	(molar ‰)	(molar)	(molar)	(molar)	(molar)	(molar)
Downstream boreholes	1	0.86	4.18	3.69E-03	4.06E-01	4.37E-01	8.63E-04	4.30E-03
	2	1.14	3.97	6.75E-03	3.73E-01	8.57E-01	3.38E-04	1.03E-02
	3	0.87	4.2	5.90E-03	4.33E-01	1.41E+00	5.79E-04	6.17E-03
	4	0.86	3.6	7.59E-03	4.19E-01	8.08E-01	4.55E-04	1.17E-02
	5	0.84	6.74	3.15E-03	5.52E-01	6.47E-01	8.12E-04	6.58E-03
	6	0.83	5.2	3.95E-03	4.71E-01	6.01E-01	9.59E-04	8.23E-03
	19	1.28	5.98	9.50E-03	7.24E-01	1.06E+00	6.00E-04	9.14E-03
	20	0.83	2.64	5.38E-03	4.88E-01	1.44E+00	2.65E-04	6.23E-03
	21	0.77	2.9	1.19E-03	2.88E-01	8.15E-01	2.93E-04	1.27E-02
	22	1.15	3.91	5.29E-03	4.52E-01	3.02E+00	2.60E-04	3.70E-02
	23	1.23	4.92	8.54E-03	7.37E-01	8.32E-01	4.47E-04	1.26E-02
	24	0.45	6.33	5.79E-03	5.71E-01	4.27E-01	7.53E-04	1.11E-02
	25	1.30	1.29	4.23E-03	3.44E-01	1.62E+00	2.52E-04	7.04E-03
26	0.81	2.89	3.82E-03	2.75E-01	1.41E+00	2.11E-04	5.34E-03	
Upstream boreholes	7	0.80	4.09	1.29E-03	6.04E-01	3.50E-01	1.00E-03	1.25E-03
	8	0.73	3.69	1.09E-03	6.00E-01	4.02E-01	7.40E-04	1.04E-03
	9	1.02	5.52	2.99E-03	4.90E-01	5.81E-01	1.17E-03	5.07E-03
	10	0.82	3.43	1.33E-03	4.86E-01	3.65E-01	8.82E-04	1.16E-03
	11	0.84	3.86	1.45E-03	6.04E-01	6.31E-01	4.60E-04	1.24E-03
	12	0.75	3.43	1.59E-03	5.07E-01	5.70E-01	4.79E-04	1.28E-03
	13	0.80	6.75	2.66E-03	5.09E-01	4.45E-01	1.48E-03	4.94E-03
	14	0.79	2.86	1.29E-03	6.09E-01	4.42E-01	9.41E-04	8.72E-04
	15	0.80	2.13	7.56E-03	5.87E-01	3.60E-01	5.59E-04	3.57E-04
	16	0.84	4.23	1.05E-03	6.92E-01	5.41E-01	4.53E-04	1.15E-03
18	1.23	8.16	2.93E-03	6.33E-01	5.89E-01	1.11E-03	6.12E-03	
Surface water	A	1.05	7.95	4.87E-03	6.52E-01	7.54E-01	2.10E-03	1.23E-02
	B	1.02	8.11	5.08E-03	6.45E-01	6.99E-01	2.41E-03	1.27E-02
	C	1.01	8.04	4.80E-03	6.45E-01	6.79E-01	2.41E-03	1.13E-02
	D	1.03	5.78	3.24E-03	6.67E-01	6.60E-01	1.69E-03	5.02E-03
	E	1.01	7.72	4.45E-03	6.55E-01	6.49E-01	2.29E-03	9.63E-03
	F	1.04	6.53	4.54E-03	6.29E-01	7.26E-01	1.90E-03	1.11E-02
	G	1.05	7.27	4.99E-03	6.34E-01	7.33E-01	2.05E-03	1.33E-02

sible contribution of fossil seawater. During dry periods (Fig. 5b), SW influence is more pronounced and all samples are near or above the seawater dilution line. The high values of B/Cl ratios are observed in the coastal sector (downstream boreholes), where a series of factors are combined and associated with anthropogenic pollution, the dissolution of evaporites and marine influence [17, 19-22].

This coastal sector presents a water table altitude below sea level during some periods, which favours marine intrusion processes attested to by Quaternary marine terraces, which are saturated by salt water [7].

The presence of bromide in groundwater is often attributed to marine aerosols. The Br/Cl ratio in water can be used to distinguish between natural and anthropogenic



Table 4. Typical ratios of major and trace elements characterizing salinity (September 2009).

	No.	Na/Cl	Sr/ Ca	B/Cl	Mg/Ca	SO <sub>4</sub> /Cl	Li/SO <sub>4</sub>	Br/Cl
		(molar)	(molar ‰)	(molar)	(molar)	(molar)	(molar)	(molar)
Downstream boreholes	1	0.79	4.35	4.41E-03	4.49E-01	4.34E-01	8.79E-04	1.35E-06
	2	1.08	4.09	6.74E-03	3.96E-01	7.66E-01	3.73E-04	1.65E-06
	3	0.86	4.28	5.84E-03	4.18E-01	1.33E+00	5.85E-04	7.63E-07
	4	0.82	2.89	5.20E-03	3.88E-01	5.94E-01	2.16E-04	1.18E-06
	5	0.85	5.07	3.43E-03	5.91E-01	6.60E-01	9.44E-04	7.65E-07
	6	0.80	5.44	4.16E-03	4.92E-01	6.01E-01	8.40E-04	8.31E-07
	19	1.02	7.7	1.32E-02	7.14E-01	8.97E-01	6.57E-04	1.56E-06
	20	0.81	3.32	3.92E-03	5.48E-01	1.02E+00	2.76E-04	7.01E-07
	21	0.78	3.06	1.28E-02	3.17E-01	8.01E-01	2.44E-04	1.48E-06
	22	0.99	8.79	1.06E-02	4.96E-01	2.55E+00	4.11E-04	6.76E-07
	23	1.18	11.01	1.84E-02	8.41E-01	7.81E-01	7.84E-04	1.74E-06
	24	0.41	13.32	1.07E-02	5.93E-01	3.62E-01	1.17E-03	7.44E-07
	25	1.18	2.94	8.98E-03	3.40E-01	2.30E+00	2.64E-04	1.40E-06
	26	0.78	8.55	9.44E-03	3.00E-01	1.35E+00	4.08E-04	1.15E-06
Upstream boreholes	7	0.85	8.51	3.16E-03	6.59E-01	4.23E+01	1.71E-03	3.72E-07
	8	0.73	8.78	2.71E-03	6.24E-01	4.03E-01	1.56E-03	3.15E-07
	9	0.75	6.7	2.33E-03	5.20E-01	2.78E-01	2.27E-03	2.93E-07
	10	0.71	7.14	2.18E-03	5.40E-01	2.91E-01	1.86E-03	3.18E-07
	11	0.80	8.58	3.30E-03	6.32E-01	6.03E-01	8.40E-04	4.22E-07
	12	0.71	8.8	3.30E-03	6.10E-01	4.89E-01	1.11E-03	4.51E-07
	13	0.74	7.35	2.48E-03	5.39E-01	3.83E-01	1.42E-03	3.32E-07
	14	0.75	7.14	2.81E-03	6.76E-01	4.58E-01	1.30E-03	4.08E-07
	15	0.89	8.29	2.18E-03	7.28E-01	5.63E-01	7.14E-04	3.46E-07
	16	0.83	6.12	2.55E-03	5.95E-01	4.05E-01	1.28E-03	4.11E-07
	18	0.77	9.72	2.84E-03	8.50E-01	5.29E-01	1.01E-03	3.36E-07
Surface water	A	0.87	8.87	2.98E-03	4.69E-01	2.23E-01	6.39E-03	2.75E-07
	B	0.88	7.96	3.09E-03	4.27E-01	1.84E-01	8.33E-03	2.83E-07
	C	0.87	8.01	2.94E-03	4.16E-01	1.67E-01	9.40E-03	2.48E-07
	D	0.86	8.15	3.13E-03	4.45E-01	1.78E-01	9.11E-03	2.60E-07
	E	0.85	7.92	2.51E-03	1.39E+00	1.40E-01	4.19E-03	1.02E-06
	F	0.87	7.82	2.94E-03	5.02E-01	2.00E-01	7.39E-03	2.74E-07
	G	0.87	3.91	1.50E-03	5.03E-01	1.87E-01	4.24E-03	2.47E-07

causes of salinization and a constant ratio shows a common origin of the two elements [23, 24]. Seawater has a constant Br/Cl molar ratio of about 1.57E-03, while Br/Cl ratio of halite is commonly lower because during evaporite deposition, halite excludes the larger Br<sup>-</sup> ion from its mineral structure. Thus, halite dissolution will produce a rapid decrease in Br/Cl ratios, while dilution of residual brines

should produce a Br/Cl ratio close to seawater or higher [19]. In the Br/Cl vs Cl diagram (Fig. 5c), during the high water period most samples of the upstream boreholes plot in the halite dissolution field, but samples of surface water, downstream boreholes and upstream 9, 13, and 18 boreholes are above the seawater dilution line, indicating a possible contribution of fossil seawater for some samples.

During low water periods most of the samples plot in the halite dissolution field (and a few groundwater samples) are near or above the seawater dilution line.

Cl, SO<sub>4</sub>, Br, B, and Li elements are often used to decipher the origin of groundwater salinity. Moreover, owing to the behavior of Li and SO<sub>4</sub> in hydrogeologic systems with potential evaporitic or deep-fluid end-members, Li/SO<sub>4</sub> ratio seems to be an interesting tool for the study of such systems. On one hand, there is Li enrichment of seawater with respect to the precipitated phases during seawater evaporation, and on the other hand, water-rock interactions at high temperatures favour Li mobility [8].

In the Li/SO<sub>4</sub> vs Cl diagrams for high and low water periods (Fig. 5d), most samples of groundwater (downstream and upstream boreholes) are near or above the seawater ratio (4.52·10<sup>-4</sup>), suggesting dissolution of evaporite as confirmed by Br/Cl and B/Cl ratios. The high values of Li/SO<sub>4</sub> ratio (higher than seawater) are observed in the river and some samples of upstream areas. These values are more elevated during low water period, suggesting that the mobilization of Li is due to the water-rock interaction at high temperatures (the presence of thermal spas in the upstream basin of Soummam).

Strontium is an element often related to evaporites. High Sr content in waters can be explained by celestite dissolution (SrSO<sub>4</sub>), a mineral commonly associated with gypsum, a relative good correlation between Sr<sup>2+</sup> and SO<sub>4</sub><sup>2-</sup> (r = 0.67), only during floods in high water periods, is observed for groundwater and suggests the dissolution of celestite as the main source of Sr<sup>2+</sup>, with this mineral often associated with gypsum, anhydrite and halite. In addition, the high correlation between Ca<sup>2+</sup> and SO<sub>4</sub><sup>2-</sup> (r = 0.88) only for high water period, suggests that another important source of Ca<sup>2+</sup> in groundwater is the dissolution of gypsum. Sr is thus a good tracer of the occurrence of evaporites. The Sr/Ca ionic ratio characteristic of an evaporitic origin is equal to or exceeds 1‰ [1, 25]. During our survey, it evolves differently according to the season (1.29-8.16 and 2.89-13.32‰). During the dry season, the strongest ratio values are observed in boreholes of the upstream part (Sidi Aich-El-Kseur) and are coupled with high sulfate, chloride, and sodium contents of these waters. The low values are located in the central part (El-Kseur-Oued Ghir), and are characteristic of waters that have flowed in the sandstone and dolomitic Triassic layers that are observed on the outcrops. In the low period, the highest values of Sr/Ca ratio are observed in the coastal area. This phenomenon can be explained by the fact that for the period of rising water level, the leaching of the evaporitic formations is mainly responsible for the salinization for all the waters of the aquifer. During the dry period, with the lowering of the water level, the marine waters participate in the salinization [2, 3].

## Conclusions

This study presents the results of several hydrochemical tracers applied for two sampling campaigns (high and low water periods). The data revealed a complex hydrogeologi-

cal system in which several sources of salinity have been identified. These can be summarized in the following way.

The chemical composition of surface and groundwater in the downstream area (along the coastal zone) of the

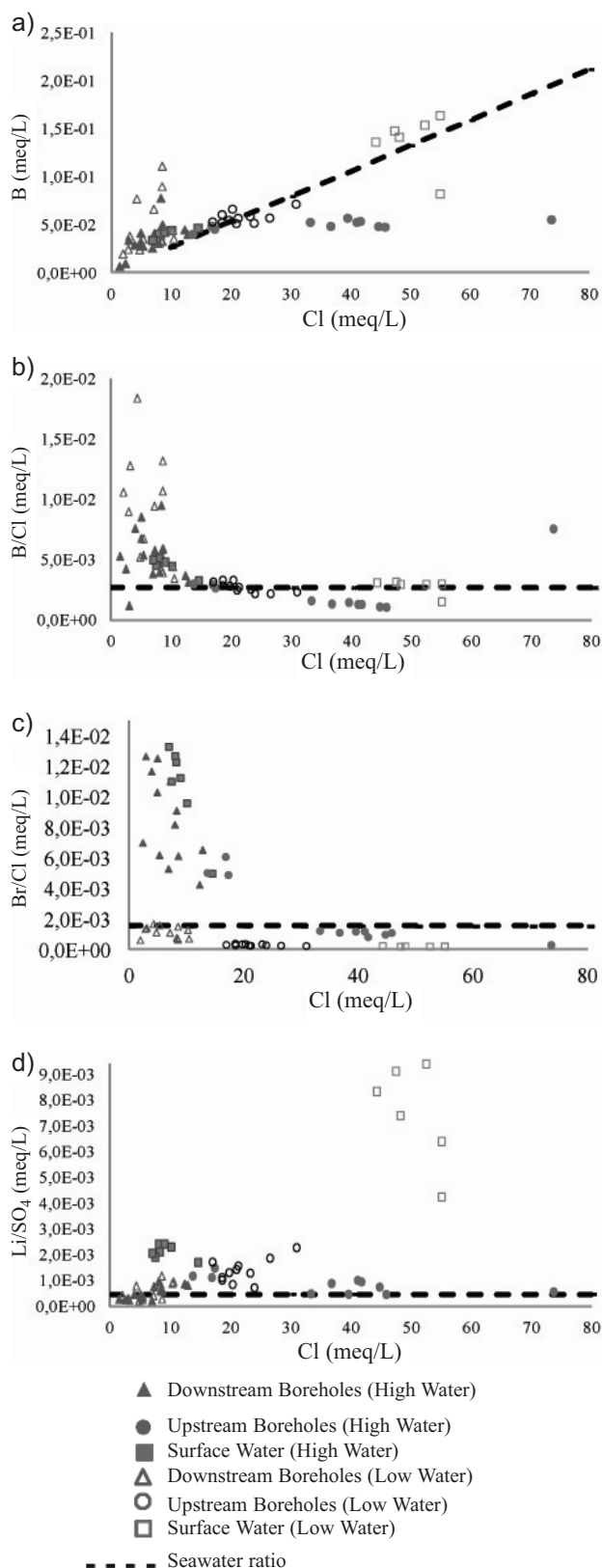


Fig. 5. Relationship between the main components characterizing the salinity of the low Soummam water (high and low water periods).

Soummam basin is characterized by low Na/Cl, SO<sub>4</sub>/Cl, and Li/SO<sub>4</sub> ratios, and high Mg/Ca, Sr/Ca, and B/Cl (lower than in seawater) ratios and a relatively high Br/Cl ratio, characteristic of seawater intrusion. In the upstream zone, with contact with Triassic formations, the chemical composition of surface and groundwater is characterized by low Na/Cl, SO<sub>4</sub>/Cl, and Br/Cl, and high Mg/Ca, Sr/Ca, and Li/SO<sub>4</sub> ratios (higher than the SW ratio = 1, 57E-03). These chemical characteristics are typical of halite and gypsum dissolution. In the central part, the chemical composition of groundwater is characterized by low Na/Cl, Sr/Ca, Mg/Ca, B/Cl, and Br/Cl ratios and relatively high SO<sub>4</sub>/Cl, and Li/SO<sub>4</sub>, characteristic of leached evaporitic rocks.

Sulphate reduction promotes the dissolution of carbonate minerals. This phenomenon could influence strongly the Mg/Ca ratio. On the other hand, the sulfate enrichment of the samples is related to the presence of evaporites in an aquifer like in the Amassine area [26, 27].

The major and trace elements commonly used for the study of saline environments (Cl<sup>-</sup>, SO<sub>4</sub><sup>2-</sup>, Mg<sup>2+</sup>, Ca<sup>2+</sup>, Br, B, Li, and Sr) confirm the role of these elements as tracers of water with evaporitic and/or marine signatures. Li/SO<sub>4</sub>, Sr/Ca, Na/Cl, B/Cl, SO<sub>4</sub>/Cl, and Br/Cl ratios are strongly relevant for the determination of water from evaporitic or marine origin.

The interpretation of the results by using the correlation of the major elements with chloride, variations of SO<sub>4</sub>/Cl, and Mg/Ca ratios showed that the downstream zone with strong salinities is contaminated by marine water and in the upstream zone by the dissolution of the evaporitic formations. Lithium and strontium data show a similar evolution of these two elements in the upstream and downstream parts of the low Soummam, but a different behavior in the coastal area. This supports the assumption of a marine influence on the one hand and the dissolution of evaporite on the other. This approach by hydrochemical tracers of a coastal aquifer with a complex geology and intense agricultural and industrial activities are made possible to highlight the contribution of several poles to chlorurated water. It was also made possible to highlight the main poles of this water type (evaporites and seawater).

A small additional Ca, SO<sub>4</sub>, and Mg due to dissolution of evaporite (only during high water period) coming from leaching of the carbonated rocks, located at the upstream basin and the salinization phenomenon occurred in the whole study area. This phenomenon suggests that calcite, dolomite, and gypsum are the minerals precipitated from evaporating seawater in the earlier stage. The process of precipitation/dissolution in the alluvial aquifer of low Soummam is confirmed by the saturation index (SI) data.

In light of this study, we can ascertain that the strong mineralization of water of the low Soummam basin has three main natural origins: evaporitic, marine, and carbonated. Upstream of the basin, from near Sidi-Aich up to the Remila River, water is sulphated, coming primarily from the basin of high Soummam and its tributaries. From the Remila River junction until Amassine, water mineralization is lower and presents a bicarbonated facies due to the con-

tributions of the northern Miocene layers. At the Amassine River junction, water again becomes sulphated, and the water is enriched in Cl and Na coming from surface waters from the Amassine River. Downstream of El-Kseur, the facies of the river banks is distinct: out of the left bank and in contact with the Miocene outcrops, water mineralization increases with a bicarbonate facies. On the right bank, water is sulphated and enriched with salts. Finally, from Oued Ghir to the sea, water is sodic chlorured and the origin of high salt content is due to marine intrusion.

### Acknowledgements

The authors wish to thank Sandra Van-Exter for her support during the laboratory work and the anonymous reviewer for comments and suggestions during the revision of the manuscript.

### References

1. ABDESLAM M., MANIA J., MUDRY J., GELARD J.P., CHAUVE P., LAMI H., AIGOUN C. Hydrogeochemical arguments for a non outcropping Triassic formation in the Djurdjura massif (kabyle ridge, an element of the Maghrebides range). *Rev. Sci. Eau*, **13**, 155, **2000**.
2. CLINCKX C. Hydrogeological study of the alluvial aquifer of the low Soummam (Sidi-Aich- Bejaia- Algeria), Algerian office of water research (D.E.M.R.H), **1973**.
3. CHEMSEDDINE F., BOUDOUKHA A., ROUABHIA A. Sources of water salinities in the Morsott-Laouinet aquifer (Northern Area of Tebessa, South East of Algeria). *Africa science*, **5**, (2), 217, **2009**.
4. VOUSTA D., DOTSIKA E., KOURAS A., POUTOUKIS D., KOUIMTZIS T.H. Study on distribution and origin of boron in groundwater in the area of Chalkidiki, Northern Greece by employing chemical and isotopic tracers. *J. Hazard. Mater.* **172**, 1264, **2009**.
5. DEBIECHE T. H. Evolution of groundwater quality (salinity, nitrogenizes and heavy metals) under the effect of pollution saltworks, agricultural and industrial, application to the low plain of Algerian north-eastern Seybouse. thesis Doct, univ Franche-Comté, pp. 199, **2002**.
6. EL YAOUTI F., EL MANDOUR A., KHATTACH A., BENAVENTE J., KAUFMANN O. Salinization processes in the unconfined aquifer of Bou-Areg (NE Morocco): A geostatistical, geochemical, and tomographic study. *Appl. Geochem.* **24**, (1), 16-31, **2009**.
7. SANCHEZ-MARTOS F., PULIDO-BOSCH A. Boron and the origin of salinization in an aquifer in Southeast Spain. *Earth Planet Sc. Lett.* **328**, 751, **1999**.
8. JALALI M. Geochemistry characterization of groundwater in an agricultural area of Razan, Hamadan, Iran. *Environ. Geol.* **56**, 1479, **2009**.
9. KAMEL S., DASSI L., ZOUARI K., ABIDI B. Geochemical and isotopic investigation of the aquifer system in the Djerid-Nefzaoua basin, southern Tunisia. *Environ. Geol.* **49**, 159, **2005**.
10. BETIER G., ROYER L., TERMIER H., LAFFITE R. Geological map (1/50.000) of Bejaia, Algerian office of geological maps., 26, **1951**.

11. DUPLAN L., GRAVELLE M. Geological map (1/50.000) of Bejaia. Algerian office of geological maps. 26, **1960**.
12. LEKINE M., GRAVELLE M., SEMROUD B. Geological map (1/50.000) of Oued Amizour, Algerian office of geological maps., 47, **1981**.
13. HERRERA L., JIMÉNEZ-ESPINOSA R., JIMÉNEZ-MILLÁN J., HISCOCK K.M. Integrate hydrochemical assessment of the Quaternary alluvial aquifer of the Guadalquivir River, southern Spain. *Appl. Geochem.* **23**, 2040, **2008**.
14. KOUZANA L., BEN MAMMOUR A., SFAR FELFOUL M. Seawater intrusion and associated processus sase of the Korba aquifer (Cap-Bon, Tunisie). *C.R. Géoscience*, **341**, (1), 21, **2009**.
15. PETALAS C., LAMBRAKIS N. Simulation of intense salinization phenomena in coastal aquifers of the thrace. *J. Hydrol.* **324**, 51, **2006**.
16. BOUCHAOU L., MICHELOT J.L., VENGOSH A., HSIS-SOU M., GAYE C.B., BULLEN T.D., ZUPPI G.M. Application of multiple isotopic and geochemical tracers for investigation of recharge, salinization, and residence time of water in the Souss-Massa. *J. Hydrol.* **352**, 267, **2008**.
17. BOUGHRIBA M., MELLOUL A., ZARHLOULE Y., OUARDI A. Spatial extension of salinization in groundwater and conceptual model of the brackish springs in the Triffa plain (northeastern Morocco). *C.R Geoscience* **338**, 768, **2006**.
18. ABDERRAHIM E., MANIA J., MUDRY J. Mechanisms of acquisitions of the mineralization of groundwater in basin Sahel-Doukkala (western Morocco) approach by hydrogeochemical tracers. *IGME Madrid*, ISBN 84-7840-470-8, **2003**.
19. FRONDINI F. Geochemistry of regional aquifer systems hosted by carbonate – evaporite formation in imbria and southern Tuscany. *Appl. Geochem.* **23**, 2091, **2008**.
20. HÉBRARD O., PISTRE S., CHEYNET N., BATIOI G.C., SEIDEL J.L. Origin of the Languedoc-Roussillon's chloride rich karstic spring waters. *C.R Geoscience* **338**, **2006**.
21. RAJMOHAN N., AL-FUTAISI A., AL-TOUQI S. Geochemical process regulating groundwater quality in a coastal region with complex contamination sources: Barka, Sultanate of Oman. *Environ. Earth Sci.*, **59**, 385, **2010**.
22. TRABELSI R., ZAIRI M., SMIDA H., BEN-DHIA H. Salinization of coastal aquifers: case of the North Sfax Sahel aquifer, Tunisia. *C.R. Géoscience*, pp. 515-524, **2005**.
23. ALCALA F.J., CUSTODIO E. Using the Cl/Br ratio as a tracer to identify the origin of salinity in aquifers in Spain and Portugal. *J. Hydrol.* **359**, 189, **2008**.
24. FAYE S., MALOSZEWSKI P., STICHLER W., TRIMBORN P., FAYE C. S., GAYE C. B. Groundwater salinization in the Saloum (Senegal) delta aquifer: minor elements and isotopic indicators. *Sci. Total Environ.* **343**, 243, **2005**.
25. BARBIERO L., REZENDE F. A., FURQUIM S.A.C., FURIAN S., SAKAMOTO A.Y., VALLES V., GRAHAM R.C., FORT M., FERREIRA R.P.D., QUEIROZ N. J.P. Soil morphological control on saline and freshwater lake hydrogeochemistry in the Pantanal of Nhecolândia, Brazil. *Geoderma* **148**, 91, **2008**.
26. FEDRIGONIA L. Origin of the salinization and hydrogeochemical behaviour of a phreatic aquifer suffering severe natural and anthropic constraints: an example from the Djebeniana aquifer (Tunisia). *Earth Planet Sc. Lett.*, **332**, 665, **2001**.
27. HSUEH Y.L., TSUNG R. P., TAI S.L. Identification of the origin of salinization in groundwater using multivariate statistical analysis and geochemical modeling: a case study of Kaohsiung, Southwest Taiwan. *Environ. Geol.* **55**, 339, **2008**.